Development of a Virtual Reality-based Power Wheel Chair Simulator

Ajay V. Sonar, Kyle D. Burdick, Ryan R. Begin, Eric M. Resch, Elizabeth M. Thompson,
Eric Thacher, Janice Searleman, George Fulk and James J. Carroll, *IEEE Member*

Department of Electrical and Computer Engineering
Wallace H. Coulter School of Engineering, Clarkson University
Potsdam, New York 13699-5720, USA

jcarroll@clarkson.edu

***Abstract*—For many individuals with physical and/or cognitive impairments the assistive technology provided by a power wheelchair (PW/C) offers the means for independent mobility, improved self-care, increased enjoyment of leisure activities and empowerment [1]. However, despite the independence afforded by a PW/C, third party payers are often reluctant to purchase a PW/C for these individuals until the person can demonstrate the ability to operate the PW/C independently. Loaner PW/C's used for training purposes are difficult to obtain and they often do not fully meet the specific needs of the client. Training methods for learning how to use a PW/C are costly and potentially unsafe. Virtual Reality technology may provide an effective training tool and method of documenting an individual's ability to operate a PW/C [2,3]. The purpose of this project is to design and build a virtual reality-based power wheelchair (VRPW/C) simulator that will provide accurate visual, proprioceptive and vestibular feedback to the user in order to accurately simulate PW/C mobility for training purposes.**

***Index Terms*—Power wheelchair, assistive technology, Stewart platform, virtual reality simulator.**

I. Introduction

Power wheelchairs (PW/C) offer the means for independent mobility for individuals with severe physical impairments thereby improving their ability to participate in society. Despite the independence afforded by a power wheelchair, third party payers are often reluctant to purchase a power wheelchair for these individuals until the person can demonstrate the ability to operate the PW/C independently. Customized PW/C can cost upwards of $15,000. This creates a classic "catch-22" scenario whereby an insurance company won't purchase a PW/C unless the individual can operate it independently but the individual does not have the opportunity to demonstrate this because they do not have a PW/C. Additionally, current training methods used to teach an individual to use a PW/C are inefficient, and potentially unsafe. Ideally, a large space is required with different environments to train in. Those users who are new to a PW/C may find it difficult to initially operate the wheelchair since they may not have adequate cognitive and/or physical ability to effectively control the PW/C.

The (VRPW/C) simulator presented in this paper may offer an alternative way to train individuals to use a PW/C and provide objective data on the client's ability to successfully operate a PW/C independently. The proposed VRPW/C offers potential benefits over traditional PW/C training methods. For example, the associated virtual environment (VE) can be shaped to meet the skill level of the client, i.e., the VE can be made easier to maneuver through at first, with the difficulty increasing as the client's ability improves. Additionally, the VRPW/C simulator can provide quantitative data on the client's performance that can be used to document change and capacity to independently operate a PW/C, e.g., for insurance purposes.

Past research, [2,4], on the application of virtual reality technology to PW/C provides both qualitative and quantitative data concerning the development and application of non-immersive virtual environments to the assessment and training of PW/C users. The developed VRPW/C system extends past results by providing users with realistic visual, kinesthetic, and vestibular feedback that is highly immersive. The system consists of three main components: (1) a seven degree-of-freedom (DOF) Stewart platform (a form of parallel robot) that serves as a motion base capable of providing haptic feedback to a user seated in a manual wheelchair mounted on the motion base that is synchronized with (2) an immersive VE, presented to a user via a stereoscopic head-mounted display (HMD), and navigated using (3) a standard PW/C control device, e.g., a joystick or puff-and-sip. The development and initial evaluation of the VRPW/C is described in detail in the remainder of the paper.

II. VRPW/C System Development

A. Overview of the VRPW/C System

Realistic PW/C simulation requires consistent visual, kinesthetic and vestibular feedback. These last two elements are made possible in the proposed VRPW/C system using a Stewart platform to manipulate a standard manual wheelchair mounted on the motion base. Visual feedback is provided by an embedded computer system mounted on the motion base. This computer outputs both visual data for a HMD, as well as

trajectory data required to servo the motion base and provide realistic kinesthetic and vestibular feedback. The trajectory data is fed to the motion base control system via a wireless network connection.

B. The Stewart Platform

The seven DOF motion base used in this application is a modified form of the Stewart platform. The Stewart platform was initially designed in 1965 and used for flight simulation [5]. The Stewart platform is a parallel manipulator that is comprised of a rigid body top plate that is connected to a bottom plate via six adjustable legs. The legs are connected to the top and bottom plates by means of universal joints. The position and orientation (or pose) of the top plate is dependent upon the length of each leg. The top and bottom plates are hexagons that are offset to each other by 60 degrees about an axis perpendicular to the ground, i.e., the z-axis. Different forms of the Stewart platform can be achieved by varying the number of distinct attachment points in the base and the top plate, as shown below in Fig. 1. The configuration used for the VRPW/C motion base has six distinct joints in the base and on the platform, and is thus termed as a type 6-6 Stewart platform.

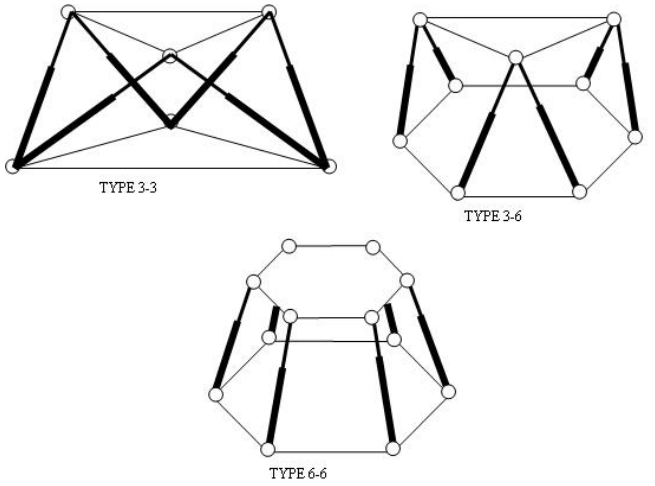

Figure 1: Stewart Platform Configurations [9].

Given the inherent limitations on its rotational range of motion, a Stewart platform alone cannot realistically simulate the physical sensations of operating a PW/C, e.g., the top plate can not produce continuous rotations. This limitation is overcome by adding a turntable to the top plate to create an additional rotational DOF. This turntable allows the motion base to rotate continuously in either direction with respect to the top plate of the Stewart platform.

All DOF of the motion base are hydraulically actuated using six cylinders one for each leg of the Stewart platform, and one motor for the turntable controlled by proportional servo valves. Feedback for the linear and rotating DOF is achieved using linear potentiometers and an incremental encoder, respectively, and facilitates precise control of the motion base pose that can quickly respond to spontaneous user movement within the virtual environment.

C. Kinematic Modeling of the Stewart Platform

Given a desired pose i.e., position and orientation, of the motion platform, the inverse kinematic model determines the manipulator variables i.e., leg positions and turntable angle, required to achieve the pose. For parallel manipulators like a Stewart platform, the development of an inverse kinematic model can be viewed as a change of coordinates. Consider the base of the platform to have coordinate system S while the top plate has coordinate system S'. The universal joint centers mounted to the bottom plate are referenced in world coordinate system S and the top universal joints referenced in the local coordinate system S'. As the top platform moves, the coordinates of the connection points never change relative to their assumed coordinate systems. As a result, the motion of S' can be viewed as a change of coordinates from S as shown below in Fig 2.

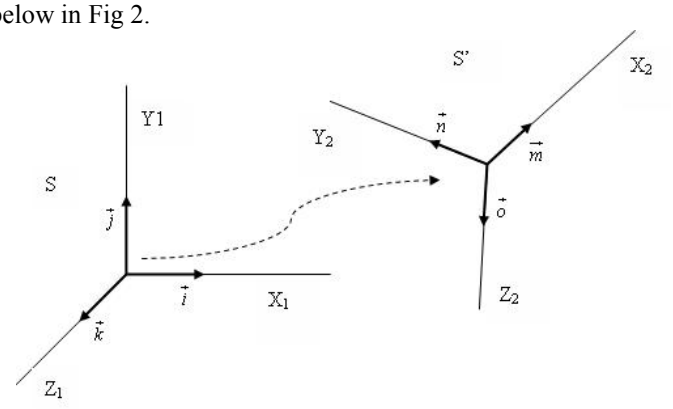

Figure 2: Change of basis for Stewart Platform.

The kinematic modeling of the Stewart platform is based on the following assumptions: (1) The universal joints are perfect, having exact centers about which perfect rotation can occur. (2) The actuators in the legs are perfect and move with only two degrees of freedom of which pass through the joint centers. (3) The leg lengths can be measured from one joint to the other without offset. (4) The top and bottom plates are carefully constructed so that the positions of the joint centers are well known.

Assume that a base coordinate frame $\{B\}$ is embedded in the base plate and a top coordinate frame $\{P\}$ embedded in the top plate. Vectors referenced in coordinate frame $\{B\}$ are denoted ${}^{B}u$, while vectors referenced in the coordinate frame $\{P\}$ are denoted ${}^{P}u$. The joints on the base are denoted by B_i, for i=1 to 6, and the position of the joint centers with respect to $\{B\}$ are given by the vectors ${}^{B}b_i = \begin{bmatrix} b_{ix} & b_{iy} & b_{iz} \end{bmatrix}^T$. Similarly, the joints on the platform are denoted P_i, for i=1 to 6, and the

position of the joint centers with respect to $\{P\}$ are given by vectors ${}^{P}p_i = \begin{bmatrix} p_{ix} & p_{iy} & p_{iz} \end{bmatrix}^T$. The six legs are denoted by L_i, with the vector from B_i to P_i defined by $\lambda_i {}^{B}l_i$, where ${}^{B}l_i = \begin{bmatrix} l_{ix} & l_{iy} & l_{iz} \end{bmatrix}^T$ is the length of leg, l_i is a direction unit vector, and the vector $\Lambda = \begin{bmatrix} \lambda_1 & \lambda_2 & \lambda_3 & \lambda_4 & \lambda_5 & \lambda_6 \end{bmatrix}^T$ describes the leg lengths. The two coordinate frames $\{B\}$ and $\{P\}$ can be related to each other through a displacement ${}^{B}q = \begin{bmatrix} x & y & z \end{bmatrix}^T$ and rotation matrix ${}^{B}R_P$:

$$ {}^{B}R_P = \begin{bmatrix} I_X & J_X & K_X \\ I_Y & J_Y & K_Y \\ I_Z & J_Z & K_Z \end{bmatrix} \quad (1) $$

The vector ${}^{B}q$ gives the relative displacement of the origin of $\{P\}$ from the origin of $\{B\}$ in terms of the x, y, and z components. The rotation matrix ${}^{B}R_P$ is composed of direction cosines defined such that a unit vector along x_P has components $\begin{bmatrix} I_x & I_y & I_z \end{bmatrix}$ in the base frame $\{B\}$, similarly a unit vector along y_P has components $\begin{bmatrix} J_x & J_y & J_z \end{bmatrix}$ in $\{B\}$ a unit vector along z_P has components $\begin{bmatrix} K_x & K_y & K_z \end{bmatrix}$ in $\{B\}$. In order to define the angles about each axis we will use Euler angle notation. This notation references rotations about the x, y and z axis as $yaw(\psi)$, $pitch(\theta)$ and $roll(\varphi)$ respectively, with these definitions ${}^{B}R_P$ can be redefined as:

$$ {}^{B}R_P = \begin{bmatrix} I_X & J_X & K_X \\ I_Y & J_Y & K_Y \\ I_Z & J_Z & K_Z \end{bmatrix} = \begin{bmatrix} c\phi c\theta & c\phi s\theta s\psi - s\phi c\psi & c\phi s\theta c\psi + s\phi s\psi \\ s\phi c\theta & s\phi s\theta s\psi + c\phi c\psi & s\phi s\theta c\psi - c\phi s\psi \\ -s\theta & c\theta s\psi & c\theta c\psi \end{bmatrix} \quad (2) $$

note: c = cosine, s = sine

The translation and rotation properties of the top plate will be combined to define a pose vector $P = \begin{bmatrix} x & y & z & \psi & \theta & \varphi \end{bmatrix}$. Let ${}^{B}u_i$ be a representation of a vector from origin $\{P\}$ to P_i, but referenced in the base frame so that:

$$ {}^{B}u_i = {}^{B}R_P \, {}^{P}p_i \quad (3) $$

Then, following the vector chain from $\{B\}$ to $\{P\}$ to P_i to B_i back to $\{B\}$ yields:

$$ {}^{B}q + {}^{B}u_i - \lambda_i {}^{B}l_i - {}^{B}b_i = 0 \quad (4) $$

Rearranging Equation 4 yields:

$$ \lambda_i {}^{B}l_i = {}^{B}u_i + {}^{B}q - {}^{B}b_i \quad (5) $$

The length of each leg can be determined by taking the Euclidean norm of Equation 5:

$$ \lambda_i = \left\| \lambda_i {}^{B}l_i \right\| = \left\| {}^{B}u_i + {}^{B}q - {}^{B}b_i \right\| \quad (6) $$

Expanding Equation 6 and squaring both sides gives:

$$ \begin{aligned} \lambda_i^2 = {} & \left[c\phi c\theta p_{ix} + (c\phi s\theta s\psi - s\phi c\psi) p_{iy} + (c\phi s\theta c\psi + s\phi s\psi) p_{iz} + x - b_{ix} \right]^2 + \\ & \left[s\phi c\theta p_{ix} + (s\phi s\theta s\psi - c\phi c\psi) p_{iy} + (s\phi s\theta c\psi - c\phi s\psi) p_{iz} + y - b_{iy} \right]^2 + \\ & \left[-s\theta p_{ix} + c\theta s\psi p_{iy} + c\theta c\psi p_{iz} + z - b_{iz} \right]^2 \end{aligned} \quad (7) $$

Equation 7 yields the leg lengths required when the pose (position and orientation) of the top plate P and the kinematics' parameters of the Stewart Platform are known.

D. Control System Design and Simulation

To accurately simulate the motion of a Stewart platform, a dynamic model must be developed based on the assumed system parameters and the desired control algorithm. While there are numerous ways to achieve this goal, one common method is to derive the dynamic equations for the Stewart platform in Cartesian coordinates using Lagrange's equations of motion as shown in [6]. This approach requires explicit calculation of the platform's forward kinematics and Jacobian matrix, a non-trivial task for Stewart platforms in general.

An alternative approach is to accurately model the Stewart Platform using a computer-aided engineering (CAE) packages that can eliminate the need to explicitly generate a mathematical model, such as: (1) MSC.Software's ADAMS/Solver or (2) the MathWork's MATLAB/Simulink. The first option uses CAD-based solid modeling techniques combined with a robust numerical analysis engine to automatically formulate and integrate the governing equations for mechanical systems undergoing large overall motion. The second option provides tools for building mechanical models that include bodies, joints, coordinate systems, and constraints that can be obtained from CAD data when combined with the SimMechanics add-on. It is possible to connect SimMechanics blocks with Simulink blocks to include nonmechanical, multidomain effects in mechanical models. This add-on integrates with the MathWork's [10] other control design and code generation products, enabling the design and real-time testing of controllers with high-level model of the mechanical systems.

For this effort, SimMechanics has been utilized given its

tight integration with the Simulink environment that permits rapid control algorithm development and auto-code generation for real-time control implementation.

The SimMechanics model used for the Stewart platform is a modified version of the model presented in [9]. The top plate, base plate and hydraulic cylinders of the Stewart platform are represented as separate bodies, as shown in Fig 3 and 4. The hydraulic cylinders consist of a top and bottom member with each link connected to the top and bottom platforms by idealized universal joints. Motion constraints are placed on each link in the SimMechanics model to restricting individual link movement to two DOF.

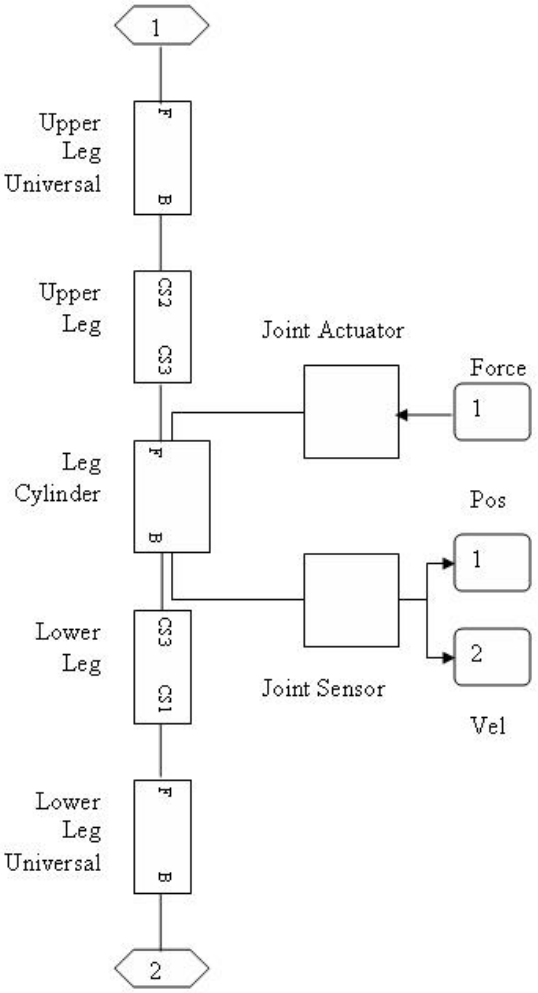

Figure 3: SimMechanics Model of a Hydraulic Cylinder.

The position of the top and bottom of each link cylinder is defined using an M-file. As these dimensions are modified, the position of the top plate is adjusted. The system dynamics are characterized by specifying various properties associated with the SimMechanic building blocks, e.g., component geometry, mass, spring and damping factors, etc. The Stewart platform model and a standard PID controller are combined to create a complete simulation model as shown below in Fig. 5.

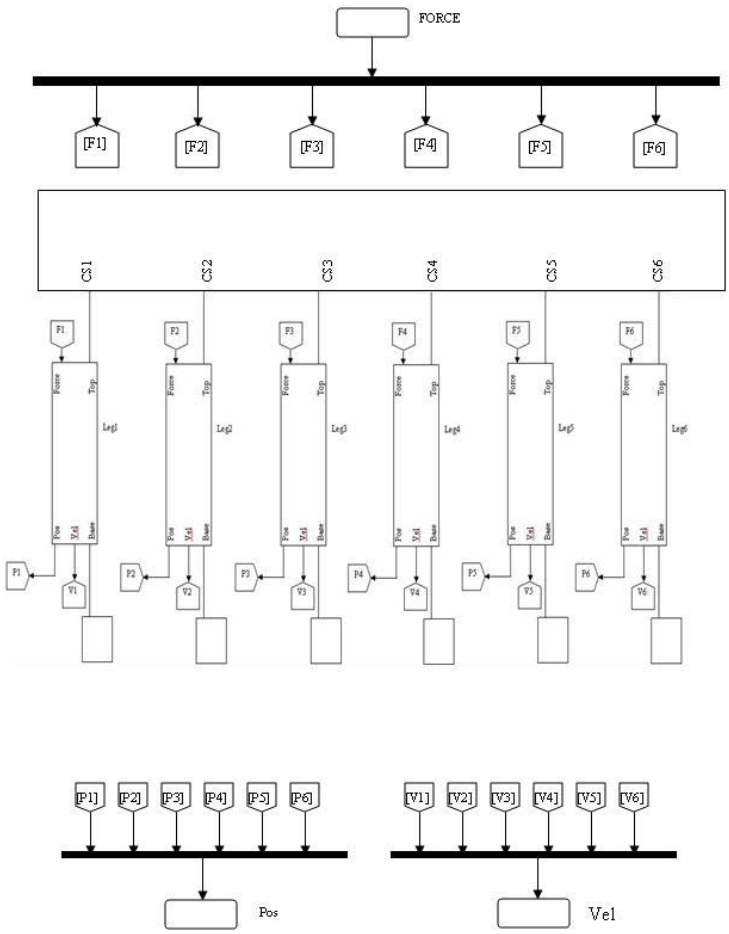

Figure 4: SimMechanics Model of the Stewart Platform.

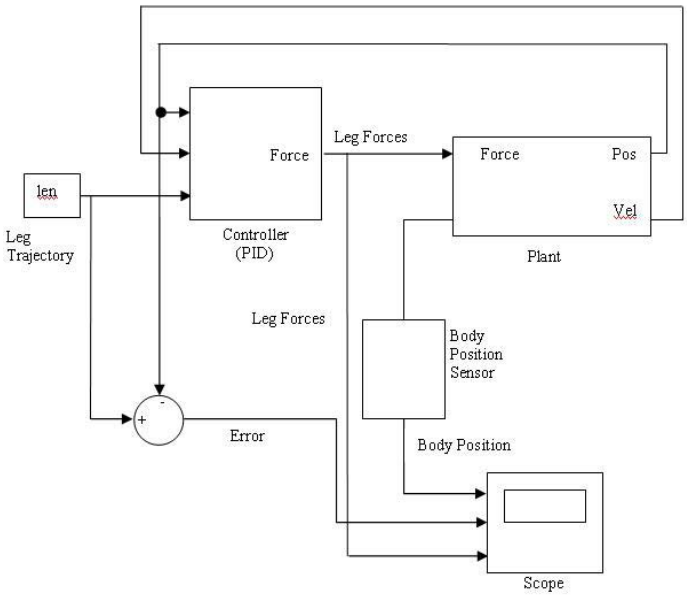

Figure 5: Complete Simulink Model of the Stewart Platform.

E. Simulation Results

The Simulink model of Fig 5 was simulated to verify the model performance and to adjust the controller gains. The

simulation results indicate that it is possible to make rapid changes in the motion base pose as required to deliver accurate haptic feedback to the VE.

F. Real-time System Implementation

The next step in the system development was to replace the simulated Stewart platform dynamics with the actual motion base. This required a computer with data acquisition capability to interface to the electromechanical components of the motion base to produce a closed-loop operation of the controller similar to that of the simulation.

The computer control system used consists of: (1) the PC-based control hardware which includes a Quanser Q8 hardware-in-the-loop PCI data acquisition and control (DAQ) board, the proportional hydraulic control valves, and the slide potentiometers and rotary encoder used to measure the leg lengths and turn table position, respectively, and (2) the control software which includes Quanser's WinCon/RTX, a real-time windows application that is compatible with the Q8 DAQ board and is capable of running the Simulink-based control code in real-time.

G.Integration Of Virtual Reality Components

To appropriately synchronize control of the motion base with wheelchair motion in the VE, an appropriate real-time data exchange between the VE and the motion base control system was necessary. This connection was made by creating a socket in the VE application (Virtools) running on the visualization PC and outputting the VE coordinate data, derived in Section I.C, directly into the MATLAB/Simulink workspace on the control PC. As the user navigates the VE, the Virtools application updates the Simulink-based controller in real-time with required platform pose information and the hydraulic legs or the Stewart platform are servoed appropriately. An image of the Stewart platform with a test user on board is shown below in Fig. 6.

Figure 6: The Stewart Platform with User on Board.

H.Safety test of the VRPW/C Simulator

Neck injuries are the most common injuries that occur when human occupants are secured to a moving object. To ensure that the VRPW/C Simulator is safe for the human operation a series of tests are performed on the simulator with test dummies strapped to it. A g-force of over 2.5 g's is an industrial standard to infer the possibility of a whip lash. The motion of the VRPW/C is controlled by Matlab code. The g-force is measured using two Analog Devices dual-axis ±5g accelerometer evaluation boards (ADXL320EB).

The first test consisted of rotating the simulator with a speed of 25 rpm while the platform remained parallel to the ground. The second test measured the g-forces resulting from maximum tilting motion at the rate of 3.5 m/s^2 along the x and y-axis. The third test is the combination of the first and second test, rotation of the platform along with the tilting motion. The fourth test was the extreme case irregular motion which combines tilting and turning of the platform in a random fashion with a maximum rate of tilting of 3.5 m/s^2 and maximum rotational speed of 25 rpm. This test was done to test the worst case scenario for experiencing a high g-force. The plots of the g-forces measured from the four tests are shown below in Fig. 7, 8, 9 and 10 respectively. The maximum g-force experienced was in the fourth test and are -0.42, 0.38 and 0.175 g's along x, y and z axis respectively. Since the data from the worst case scenario yielded a maximum g-force at 1/5 of that of the allowed g-force it is inferred that the VRPW/C is safe for human use.

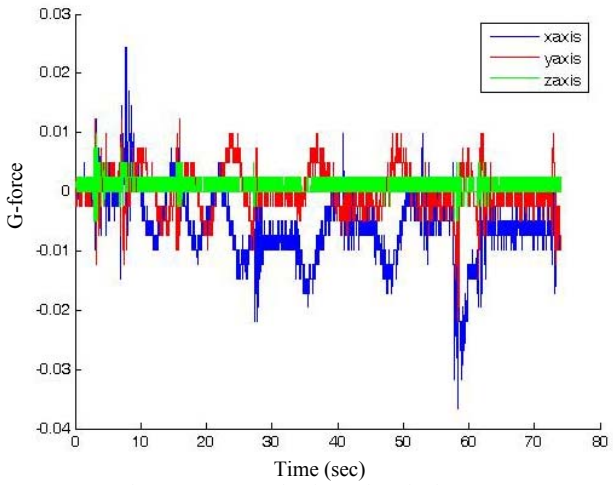

Figure 7: Measured g-forces in spinning test

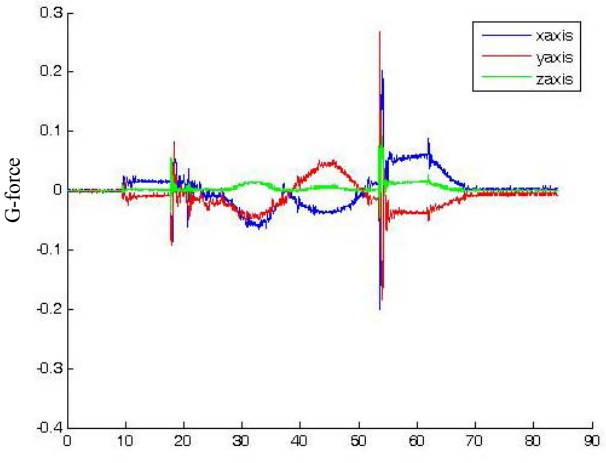

Figure 8: Measured g-forces in tilting test

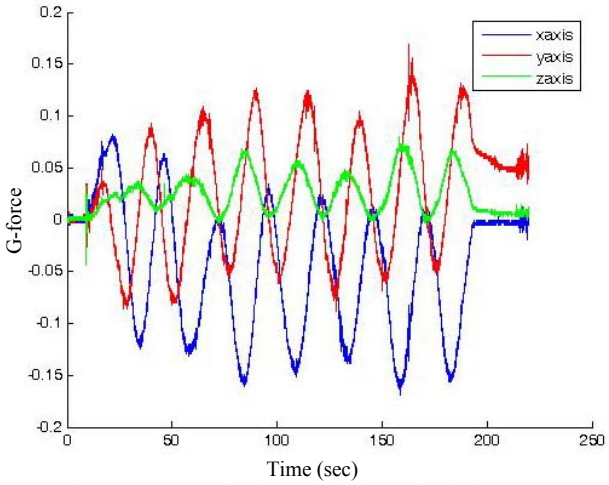

Figure 9: Measured g-forces in tilting and spinning test

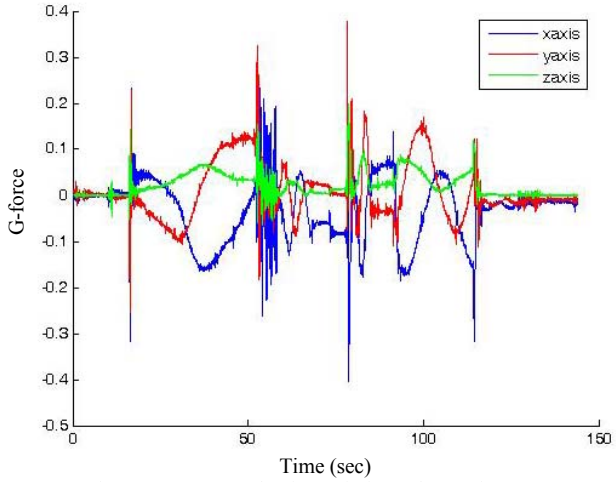

Figure 10: Measured g-forces in irregular motion test

III. THE VIRTUAL ENVIRONMENT

The two aspects of the virtual environment are the modeling of the environment and real-time simulation/display. The entire modeling of the environment is done in 3D Studio Max [11]. The model was then exported to Virtools [12] for real-time simulation/display. The PW/C dynamics are simulated using a model developed using the Virtools Physics Pack. A PW/C joystick is used to navigate the VRPW/C. The rear wheels are controlled by two individual motors that are created in the Physics Pack. The front wheels are attached by a set of casters and are free to rotate about their axis (X-axis in Virtools) and also about the vertical axis (Z-axis in Virtools) as shown in Fig. 11. The view as seen by the user's perspective in Virtools is shown in Fig. 12.

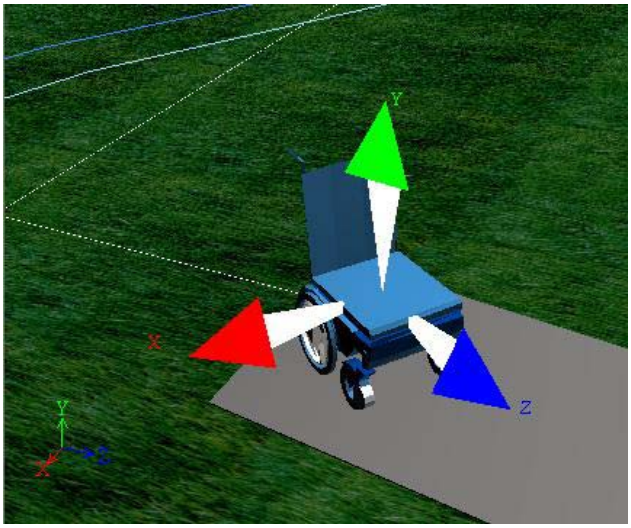

Figure 11: Model of the wheelchair.

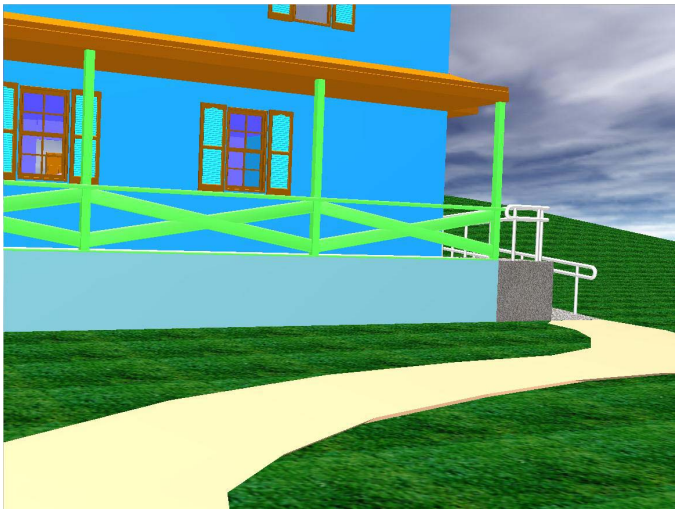
Figure 12: View as seen by the PW/C user's perspective.

The VE is displayed on a head-mounted display (HMD) worn by the user. The HMD used is an I-Visor DH-4400VPD capable of stereoscopic display i.e., a separate left and right image of the VE. The orientation of the head is tracked by an Intrersense InterTrax2 3-DOF angular tracker mounted on the HMD. The tracking information is sent to a camera in the

Virtools VE, which is used to display the VE from the user's perspective. The camera tracks the orientation of the user's head and in turn changes the view on the HMD accordingly. Thus, when the user turns his/her head to the left, the camera rotates to the left by the same amount appropriately changing the view on the HMD.

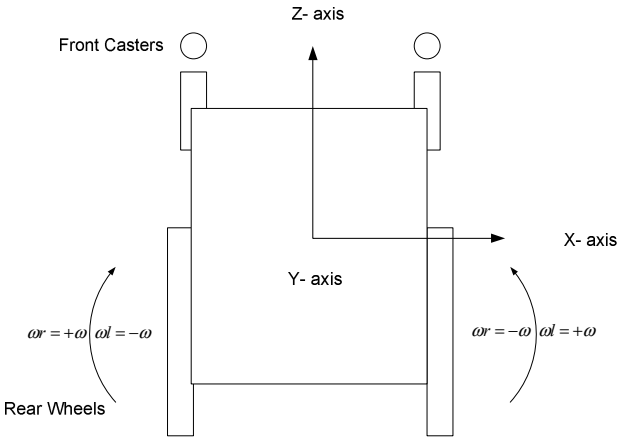

Figure 13: Diagram of the wheelchair.

Fig. 13 shows a diagram of the wheelchair model along with the angular velocities for the rear wheels while turning right, left and moving straight ahead. When the wheelchair is moving forward with the wheels rotating at ω rad/sec the rotation of the back-left wheel (ω_{bl}) and the rotation of the back-right wheel (ω_{br}) are given by

$$\omega_{bl} = \omega_{br} = +\omega \tag{8}$$

For wheelchair moving backwards

$$\omega_{bl} = \omega_{br} = -\omega \tag{9}$$

For wheelchair taking a left turn

$$\omega_{bl} = -\omega \text{ and } \omega_{br} = \omega \tag{10}$$

For wheelchair taking a left turn

$$\omega_{bl} = \omega \text{ and } \omega_{br} = -\omega \tag{11}$$

Fig 14 below shows the implementation of equations (8), (9), (10) and (11) in Virtools using elements of the Physics Pack.

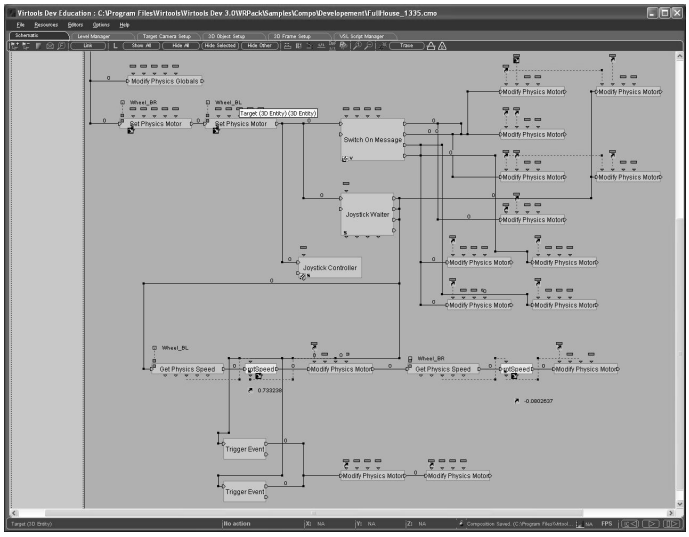

Figure 14: The Virtools Script for Navigation of the Wheelchair in the VE.

The front caster orientation influences the reverse directional stability of the PW/C. The Virtools model of the PW/C is simulated using the front caster orientations of Fig. 15. The results, shown in Fig 16, compare favorably to the experimental measurements made on actual wheelchairs, as published by Ding, et. al [7]

IV. Conclusion

The experimental setup described is a first step towards the development of a system capable of generating realistic haptic feedback for PW/C simulation. It uses a Stewart platform system in combination with an immersive VE. The accuracy of the VE has been tested in terms of wheelchair stability and found to compare favorably with other published results. Future work includes further development and refinement of the VE, e.g., to include a wider variety of daily living activities, and the clinical testing to see how VRPW/C training compares to traditional PW/C training techniques.

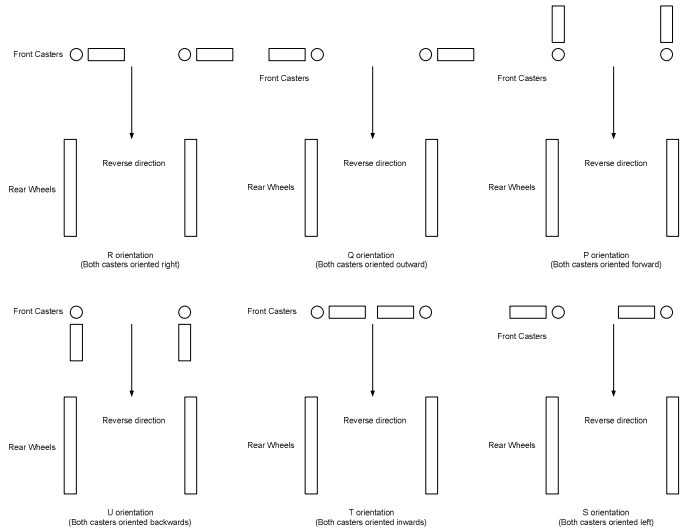

Figure 15: Six Different Initial Front Caster Orientations.

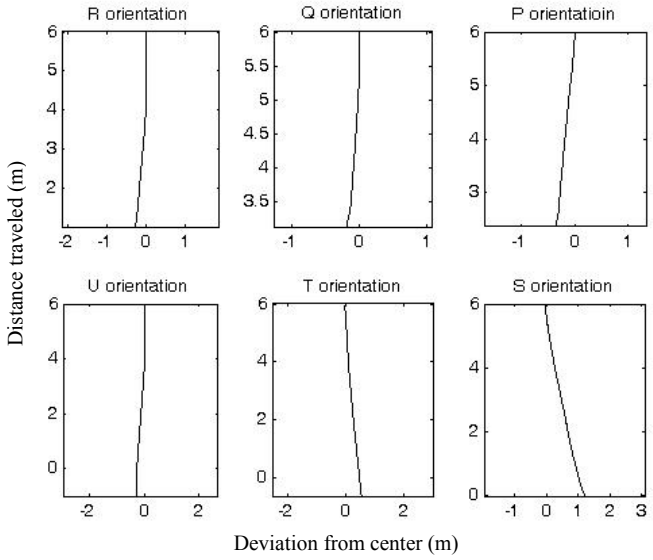

Figure 16: Path of Wheelchair Moving Backward with 6 Front Caster Orientations for the Wheelchair Speed of 1m/s.

ACKNOWLEDGMENT

The authors would like to thank their undergraduate student colleagues who have contributed to the initial success of this work and Mr. Bruce Stowell for his support in assembling the system hydraulics.

REFERENCES

[1] C. Miles-Tapping, "Power Wheelchairs and Independent Life Styles," *Can Journal Rehabil*., Vol. 10, No. 2, pp.137-145, 1996.

[2] A. Harrison, G. Derwent, A. Enticknap, F. D. Rose and E. A. Attree "Application of Virtual Reality Technology to the Assessment and Training of Powered Wheelchair Users", Proc. 3rd Intl Conf. Disability, Virtual Reality and Assoc. Tech., Alghero, Italy (2000).

[3] A. Hasdai, A. S. Jessel, and P. L. Weiss, "Use of a Computer Simulator for Training Children With Disabilities in the Operation of a Powered Wheelchair," *Am J Occup Ther*., Vol. 52, pp. 215-220, 1998.

[4] H. Niniss and A. Nadif, "Simulation of the behavior of a powered wheelchair using virtual reality", *Proc. 3rd Intl Conf. Disability, Virtual Reality and Assoc. Tech*., Alghero, Italy 2000.

[5] V. De Sapio, "Some Approaches for Modeling and Analysis of a Parallel Mechanism with Stewart Platform Architecture," *Sandia National Laboratories Technical Report,* No. SAND98-8242, May 1998.

[6] K. Liu, D. M. Dawson, and F. L. Lewis, "Modeling and Control of a Stewart Platform Manipulator," *ASME Winter Annual Meeting, Atlanta,* GA., DSC-Vol. 33, 1991, pp 83-89.

[7] D. Ding, Member, R. A. Cooper, S. Guo and T. A. Corfman, "Analysis of Driving Backward in an Electric-Powered Wheelchair", *IEEE Transaction on Control Systems Technology*, VOL. 12, NO. 6, November 2004.

[8] H. Asada and J.J.E. Slotine, *Robot Analysis and Control*, John Wiley and Sons, 1986.

[9] MATLAB Digest, Vol. 10, No. 5, September 2002.

[10] www.mathworks.com

[11] www.discreet.com

[12] www.virtools.com